DLES7: Direct and Large-Eddy Simulations 7, Edited by V. Armenio, B. Geurts and J. Fröhlich
Springer, ERCOFTAC Series, Vol. 13. pp. 261–266, 2010

A dissipative scale-similarity model.

L. Davidson

Division of Fluid Dynamics, Dept. of Applied Mechanics, Chalmers University of Technology, Gothenburg, Sweden lada@chalmers.se

1 The dissipative scale-similarity model

When the first scale-similarity model was proposed it was found that it is not sufficiently dissipative [1]. An eddy-viscosity model has to be added to make the model sufficiently dissipative; these models are called *mixed* models. The present work presents and evaluates a new dissipative scale-similarity model.

The filtered Navier-Stokes read

$$\frac{\partial \bar{u}_i}{\partial t} + \frac{\partial}{\partial x_k}(\bar{u}_i \bar{u}_k) + \frac{1}{\rho}\frac{\partial \bar{p}}{\partial x_i} = \nu \frac{\partial^2 \bar{u}_i}{\partial x_k \partial x_k} - \frac{\partial \tau_{ik}}{\partial x_k}, \quad \frac{\partial \bar{u}_i}{\partial x_i} = 0 \tag{1}$$

where τ_{ik} denotes the SGS stress tensor. In the scale-similarity model, the SGS stress tensor is given by

$$\tau_{ik} = \overline{\bar{u}_i \bar{u}_k} - \bar{\bar{u}}_i \, \bar{\bar{u}}_k \tag{2}$$

This model is not sufficiently dissipative. Let us take a closer look at the equation for the resolved, turbulent kinetic energy, $K = \langle u_i' u_i' \rangle / 2$ (where $u_i' =$

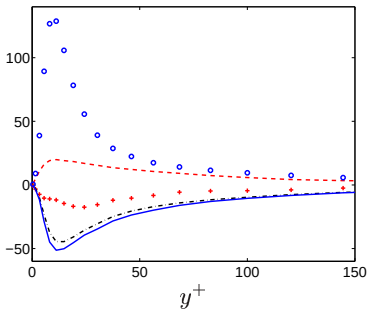

Fig. 1. Dissipation terms and production term from channel flow DNS data. 96^3 mesh data filtered onto a 48^3 mesh. $Re_\tau = 500$. —— : $-\varepsilon^+_{SGS}$; - - - : $-\varepsilon^-_{SGS}$; - · - : $-\varepsilon^D_{SGS}$ (see Eq. 6); ∘: $-\langle u'v' \rangle \partial \langle U \rangle / \partial y$; +: $-\varepsilon_{SGS}$.

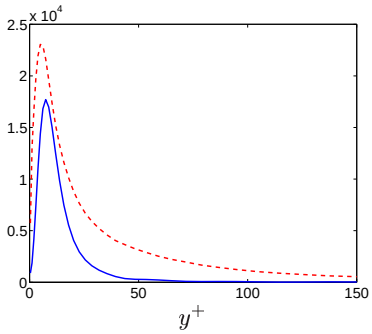

(a) ——— : $\left|\partial^2\langle\bar{u}\rangle/\partial y^2\right|$; - - - : $RMS(\partial^2 u'/\partial y^2)$.

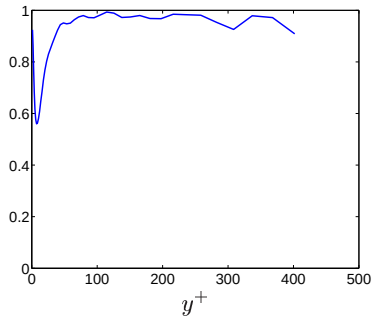

(b) Correlation coefficient of $\partial^2 u'/\partial y^2$ and $\partial^2\bar{u}/\partial y^2$.

Fig. 2. Channel flow DNS data from a 96^3 grid filtered to 48^3. $Re_\tau = 500$.

$\bar{u}_i - \langle\bar{u}_i\rangle$), which reads

$$\frac{\partial K}{\partial t} + \frac{\partial}{\partial x_i}(\bar{u}_i K) + \langle u_k' u_i'\rangle\frac{\partial\langle\bar{u}_i\rangle}{\partial x_k} + \frac{\partial\langle p' u_i'/\rho\rangle}{\partial x_i} + \frac{1}{2}\frac{\partial\langle u_k' u_i' u_i'\rangle}{\partial x_k} = \nu\left\langle\frac{\partial^2 u_i'}{\partial x_k\partial x_k}u_i'\right\rangle -$$
$$\left\langle\left(\frac{\partial\tau_{ik}}{\partial x_k} - \left\langle\frac{\partial\tau_{ik}}{\partial x_k}\right\rangle\right)u_i'\right\rangle = \nu\left\langle\frac{\partial^2 u_i'}{\partial x_k\partial x_k}u_i'\right\rangle - \left\langle\frac{\partial\tau_{ik}}{\partial x_k}u_i'\right\rangle = \tag{3}$$
$$\nu\frac{\partial^2 K}{\partial x_k\partial x_k} - \underbrace{\nu\left\langle\frac{\partial u_i'}{\partial x_k}\frac{\partial u_i'}{\partial x_k}\right\rangle}_{\varepsilon} - \underbrace{\left\langle\frac{\partial\tau_{ik}}{\partial x_k}u_i'\right\rangle}_{\varepsilon_{SGS}}$$

The first term on the last line is the viscous diffusion term and the second term, ε, is the viscous dissipation term which is always positive. The last term, ε_{SGS}, is a source term arising from the SGS stress tensor, which can be positive or negative. When it is positive, forward scattering takes place (i.e. it acts as a dissipation term); when it is negative, back scattering occurs.

Figure 1 presents SGS dissipation, ε_{SGS} in Eq. 3, computed from filtered channel flow DNS data. The forward scatter, ε^+_{SGS}, and back scatter, ε^-_{SGS}, SGS dissipation are defined as the sum of all instants when ε_{SGS} is positive and negative, respectively. As can be seen, the scale-similarity model is slightly dissipative (i.e. $\varepsilon_{SGS} > 0$) , but the forward and back scatter dissipation are both much larger than ε_{SGS}.

One way to make the SGS stress tensor strictly dissipative is to set the back scatter to zero, i.e. $\max(\varepsilon_{SGS}, 0)$. This could be achieved by setting $\partial\tau_{ik}/\partial x_k = 0$ when its sign is different from that of u_i' (see the last term in Eq. 3). This would work if we were solving for K. Usually we do not, and the equations that we do solve (the filtered Navier-Stokes equations) are not directly affected by the dissipation term, ε_{SGS}.

Instead we have to modify the SGS stress tensor as it appears in the filtered Navier-Stokes equations, Eq. 1. The second derivative on the right side is usually called a *diffusion* term because it acts like a diffusion transport term. When analyzing the stability properties of discretized equations to an imposed disturbance, u', using Neumann analysis (see, for example, Chapter 8 in [2]), this term is referred to as a *dissipation* term. In stability analysis the concern is to dampen numerical oscillations; in connection with SGS models, the aim is to dampen turbulent resolved fluctuations. It is shown in Neumann analysis that the diffusion term in the Navier-Stokes equations is dissipative, i.e. it dampens numerical oscillations. However, since it is the resolved *turbulent fluctuations*, i.e. K in Eq. 3, that we want to dissipate, we must consider the filtered Navier-Stokes equations for the fluctuating velocity, u_i'. It is the diffusion term in this equation which appears in the first term on the right side (first line) in Eq. 3. To ensure that $\varepsilon_{SGS} > 0$, we set $-\partial\tau_{ik}/\partial x_k$ to zero when its sign is different from that of the viscous diffusion term (cf. the two last terms on the second line in Eq. 3). This is achieved by defining a sign function

$$M_{ik} = \text{sign}\left(-\frac{\partial\tau_{ik}}{\partial x_k}\frac{\partial^2 u_i'}{\partial x_k \partial x_k}\right), \text{no summation on } i,k \tag{4}$$

where $M_{ik} = \pm 1$. The problem is that we do not know u_i' $(= \bar{u}_i - \langle\bar{u}_i\rangle)$ until the simulations have been carried out. Fortunately, the sign of the second derivative of the resolved velocity fluctuation, u_i', is mostly the same as that of the resolved velocity, $\bar{u}_i$. Figure 2(a) presents a comparison of the two second derivatives using channel flow DNS data from a 96^3 grid filtered onto a 48^3 grid. As can be seen, the RMS of the second derivative of u' is larger – or much larger – than that of $\langle\bar{u}\rangle$. Figure 2(b) shows the correlation of the signs of the two second derivatives. It can be seen that the correlation is larger than 95% for $y^+ > 40$. Hence Eq. 4 can be replaced by

$$M_{ik} = \text{sign}\left(-\frac{\partial\tau_{ik}}{\partial x_k}\frac{\partial^2 \bar{u}_i}{\partial x_k \partial x_k}\right), \text{no summation on } i,k \tag{5}$$

Each component of the divergence of SGS stress tensor in Eq. 1 is then simply multiplied by $\tilde{M}_{ik} = \max(M_{ik}, 0)$ i.e.

$$\frac{\partial\tau_{ik}^D}{\partial x_k} = \tilde{M}_{ik}\frac{\partial\tau_{ik}}{\partial x_k}, \text{no summation on } i,k \tag{6}$$

The SGS dissipation, $\varepsilon_{SGS}^D = \langle(\partial\tau_{ik}^D/\partial x_k)u_k'\rangle$ (cf. Eq. 3), is shown in Fig. 1.

It should be noted that, since the limiter $\tilde{M}_{ik}$ operates on each cell rather than on each face, the SGS diffusive fluxes, τ_{ik}^D, are not conservative. However, this is unavoidable since we need to control the *net* force per unit volume, $\partial\tau_{ik}^D/\partial x_k$, rather than the stresses at the face, τ_{ik}^D. It could also be mentioned that $\partial\tau_{ik}^D/\partial x_k$ is not coordinate invariant; however, this feature is shared by

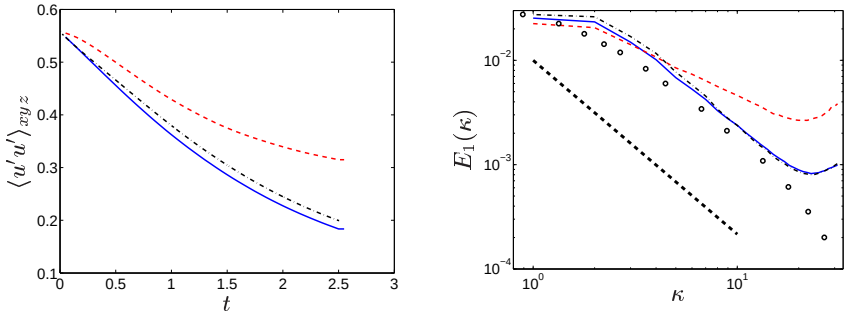

Fig. 3. Decaying isotropic grid turbulence. —— : Dissipative scale-similarity model; - - - : scale-similarity model; - - - : Smagorinsky model ($C_S = 0.14$); ∘ experiments [3]. Left: Decaying of $\langle u'u' \rangle_{xyz}$ versus time; right: Longitudinal one-dimensional spectra.

most bounded discretization schemes where numerical limiters are used for the convective fluxes.

It can be noted that by using Eq. 5 rather than Eq. 4 the model is no longer strictly dissipative in the $K = \langle u_i' u_i' \rangle / 2$ equation. It is now only 95% dissipative, see Fig. 2(b). However, the model is – assuming that the diffusion term $\nu \partial^2 K / \partial x_j \partial x_j$ in Eq. 3 is negligible – indeed strictly dissipative in the $\langle \bar{u}_i \bar{u}_i \rangle / 2$ equation.

In order to avoid that the sign function changes sign between two iterations within a time step, the second derivatives in Eq. 5 are evaluated using velocities at the old time step.

By using the limiter $\tilde{M}_{ik}$ we omit the back scatter caused by the SGS stresses; another way to express it is that we exclude the part of the subgrid stress stress term that acts as *counter-gradient* diffusion.

2 Results

2.1 Decaying grid turbulence

The domain is a cubic box of side 4π covered by 64 cells. Figure 3a presents the decay of the turbulent resolved fluctuations versus time and Fig. 3b compares the predicted one-dimensional energy with experimental data. The pile-up of energy at the small scales exhibited by all models occurs because the smallest scales cannot be resolved by the grid. As can be seen, both the decay and the one-dimensional spectrum obtained with the dissipative scale-similarity model are very similar to those obtained with the Smagorinsky model. It can also be seen that the dissipative model is indeed much more dissipative than the original scale-similarity model.

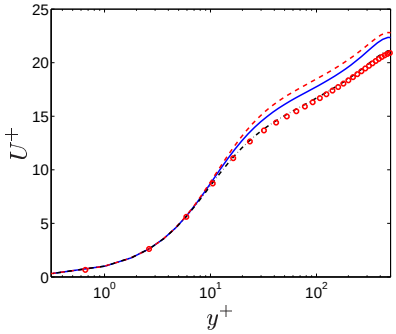

Fig. 4. Channel flow. —— : Dynamic model; - - - dissipative scale-similarity model. - . - . - : no model; ○: DNS [4].

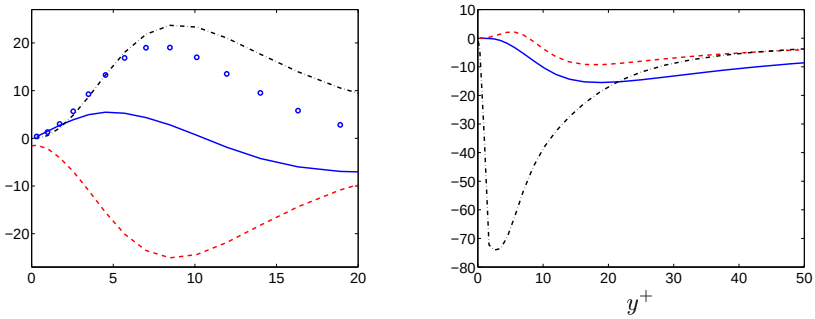

(a) —— : $-5 \cdot \partial\langle\tau_{12}^D\rangle/\partial y$; - - - : $\nu\partial^2\langle\bar{u}\rangle/\partial y^2$; - . - . - : $-\partial\langle u'v'\rangle/\partial y$; ○: $-5 \cdot \partial\langle\tau_{12}\rangle/\partial y$.

(b) —— : $-\langle u_i'\partial\tau_{ik}^D/\partial x_k\rangle$; - - - : $-\langle u_i'\partial\tau_{ik}/\partial x_k\rangle$; - . - . - : $-2\langle\nu_{smag}s_{ij}'s_{ij}'\rangle$ ($C_s = 0.1$).

Fig. 5. a) Terms in the momentum equation. b) Terms in the K equation.

2.2 Fully developed channel flow

The Reynolds number is 500 based on the half channel height and the friction velocity. The mesh has $64 \times 80 \times 64$ (x, y, z) cells. The extent of the computational domain is 3.2 and 1.6 in the streamwise (x) and spanwise (z) directions, respectively. A grid stretching of 12% is used in the wall-normal direction.

Figure 4 presents the velocity profiles obtained with the dissipative scale-similarity model, the dynamic model and with no model. No converged results could be obtained with the standard scale-similarity model. As can be seen, no model gives perfect agreement with DNS and the log-law. Hence, this flow is not a good test case for evaluating the accuracy of SGS models. Here it is used to analyze the dissipative scale-similarity model. The dynamic model gives slightly better agreement with DNS than the dissipative scale-similarity model.

Figure 5(a) presents the momentum diffusion terms close to the wall. It can be seen that the SGS diffusion term evaluated using the standard scale-similarity model is of opposite sign to that of the viscous diffusion. When introducing the sign function in Eqs. 4 and 5, it can be seen that the SGS diffusion term takes the same sign as the viscous diffusion term for $y^+ > 10$. The fact that the two terms have opposite signs for $y^+ < 10$ simply means that the viscous diffusion is very large at instants when the SGS diffusion term is set to zero. The diffusion due to the resolved shear stress is included in the figure. It is, as can be seen, much larger (more than five times) than the SGS term.

Figure 5(b) compares the SGS dissipation from the scale-similarity model with that from the dissipative scale-similarity model (recall that the simulation was carried out with the latter model). As can be seen, the SGS dissipation is indeed much larger with the dissipative model than with the standard model. For comparison, the SGS dissipation, ε_{smag}, is also included.

3 Concluding Comments

In the proposed new scale-similarity model the back scatter generated by the model is omitted. An alternative way to modify the scale-similarity model is to omit the *forward* scatter, i.e. to include instants when the subgrid stresses act as *counter-gradient* diffusion. In hybrid LES-RANS, the stresses can then be used as forcing at the interface between URANS and LES. This new approach is the focus of [5].

Acknowledgements

The financial support of SNIC (Swedish National Infrastructure for Computing) for computer time at C3SE (Chalmers Center for Computational Science and Engineering) is gratefully acknowledged.

References

1. J. Bardina, J.H. Ferziger, and W.C. Reynolds. Improved subgrid scale models for large eddy simulation. AIAA 80-1357, Snomass, Colorado, 1980.
2. C. Hirsch. *Numerical Computation of Internal and External Flows: Fundamentals of Numerical Discretization*, volume 1. John Wiley & Sons, Chichester, UK, 1988.
3. G. Comte-Bellot and S. Corrsin. Simple Eularian time correlation of full- and narrow-band velocity signals in grid-generated "isotropic" turbulence. *Journal of Fluid Mechanics*, 48(2):273–337, 1971.
4. J.C. del Alamo and J. Jimenez. Spectra of the very large anisotropic scales in turbulent channels. *Physics of Fluids A*, 15(6):L41–L44, 2003.
5. L. Davidson. Hybrid LES-RANS: back scatter from a scale-similarity model used as forcing. *Phil. Trans. of the Royal Society A*, 367(1899):2905–2915, 2009.